ELBA BIOFLUX

Extreme Life, Biospeology & Astrobiology
International Journal of the Bioflux Society

Analysis and adsorption-interaction of amino acids on basaltic mineral subjected to different simulated atmospheres

[1,4]Emmanuel A. Lalla, [2]Eva Mateo Martí, [3,4]Jesús Medina, [2,3,4]Antonio Sansano, [2,3,4]Aurelio Sanz-Arranz, [4,5]Jesús Martínez-Frías, and [2,3,4]Fernando Rull Perez

[1] Department of Physics, University of La Laguna, Tenerife, Spain; [2]Centro de Astrobiología CSIC-INTA, Torrejón de Ardoz, Madrid, Spain; [3]Department of Condensed Matter Physics, Crystallography and Mineralogy, University of Valladolid, Valladolid, Spain; [4]Unidad Asociada Uva-CSIC- al Centro de Astrobiología CSIC-INTA "ERICA", Valladolid, Spain; [5]Department of Earth Dynamics and Observation, Instituto de Geociencias, IGEO (CSIC-UCM), Madrid, Spain. Corresponding author: Emmanuel A. Lalla, emmanuellalla@gmail.com

Abstract. The research have been conducted in order to have a better understanding of amino acid adsorption on volcanic matrix surface subjected to different extreme environmental conditions (Martian surface environment, space environment, UV-environment, etc.) simulated by The Planetary Atmosphere and Surfaces Chamber (PASC) at the "INTA-Centro de Astrobiogia". The spectroscopic measurements were done by Raman and IR spectroscopy (at the Unidad Asociada Uva-CSIC at Centro de Astrobiología) taking into account the capabilities of the combined Raman-IR analyses for astrobiological target such as the detection of biomarkers on the future ESA-ExoMars Mission. Moreover, SEM-EDX analyses have been conducted in order to complement the spectroscopic results, which endeavour the use of spectroscopic systems for space missions. Conclusion: The L-aspartic acid shows to be the most suitable amino acid for this kind of experiment; the amino acid half–life is 10^4 seconds according to the reference; both spectroscopic techniques, working in synergy, have detected the amino acid degradation, but amino acid mineral interaction was not detected; the experiments have shown the versatility of the simulation chamber (PASC) to perform experiments under different planetary environments.
Key Words: Amino acids, Raman Spectroscopy, IR spectroscopy, Martian environment, Simulation Chambers.

Resumen. Los experimentos se han realizado con el objetivo de tener un mejor entendimiento sobre aminoácidos inmovilizados sobre matrices de caracter volcánico y estos han sido sometidos a diferentes ambientes extremos (Ambiente marciano, ambiente espacial, ambiente de radiación UV, etc.) dentro de la Cámara de Simulación de atmosferas y superficies planetarias (PASC) en el Centro de Astrobiología-INTA. Los métodos espectroscópicos usados son la espectroscopía Raman e Infrarroja (en la Unidad Asociada Uva-CSIC al Centro de Astrobiología) teniendo en cuenta las capacidades combinadas de estos sistemas para objetivos astrobiológicos como la detección de biomarcadores en la futura misión ESA-ExoMars. Además, se realizaron medidas mediante microscopía electrónica (SEM-EDX) las cuales complementan los resultados espectroscópicos y refuerzan el uso de estos sistemas para misiones espaciales. Conclusiones: El ácido L-Aspartico demostró ser el más eficiente para este tipo de experimentos; la vida media de los aminoácido es de 10^4 teniendo en cuenta las referencias; ambos sistemas espectroscópicos Raman-IR, trabajando conjuntamente, detectaron la degradación de los aminoácidos, pero la interacción entre aminoácido-mineral no fue detectada; los experimentos demostraron la versatilidad de la Cámara de Simulación (PASC) en cuanto a la realizacion de experimentos en distintos ambientes planetarios.
Palabras Clave: Aminoácidos, Espectroscopía Raman, Espectroscopia Infrarroja, Ambiente Marciano, Cámaras de Simulación.

Introduction. In Astrobiology, the searching of life has determined the scientific community to think about the possibility to find rests of past or present life on Mars. This may be concluded through the data obtained from orbiters and rovers, which indicate the existence of liquid water in significant amounts on Mars in the past and the possibility of important biological reactions. On the other hand, the data obtained have also shown

that Mars had an important volcanic activity in the past, where about the 90% of the material comes from igneous activity on Mars (Zorzano et al 2009). Moreover, the successful detection of the enantiomeric excess of amino acids in the Murchison and Murray meteorites, which have a volcanic origin, in the related literature, has been discussed, where the possibility of survival of amino acids and organic molecules in the Martian regolith could have occurred (Berger 2003; Gómez et al 2010; Izumi et al 2008; Sánchez et al 2012). The correct selection of natural samples from basaltic terrestrial analogues have been done considering the volcanic behaviour. Thus, the Tenerife Island outcrops are an areas of reference for carrying out research and technological studies with planetary and astrobiological implications. Several places of the Island have been selected considering the relevant volcanic activity and episodes: the fluid-rock interactions caused by the weathering processes, the submarine, subaerial and hydrothermal alterations (Lalla 2014).

However, there is a lack of information on experiments based on basalt or igneous material. Thus, the study of the degradation and stability of organic material on basalt and igneous material exposed to Martian conditions and other simulated atmospheres on basalt and igneous material would help us to understand the stability of amino acids in extreme conditions (Ten Kate et al 2005).

The way to achieve the Martian conditions on Earth is by a simulation chambers, which is a platform that allows us to reproduce planetary and interstellar conditions like the Moon and Martian environment conditions (Caro et al 2006) . But the space simulations also cover other objectives, such as the understanding of the results obtained in space missions and the preparation of the new space missions, which are extremely important for the technological point of view. The simulation chambers have an important role for testing and calibrating the best way under similar operating conditions of the implementation with those on the missions. Thus, the future successful performance of the space missions is enforced (Mateo-Marti 2014; Waiters 2003).

The future ExoMars space mission, composed principally by a landing module with an autonomous rover, equipped with an automatic laboratory *Drawler* (see Figure 1-A), will be able to provide exobiological data as well as its contextual information from the red planet. But the search of signs of microbial life - past or present - on the Martian surface and subsurface is not the only objective, since the results are going to improve our knowledge of the past/present geochemistry, water distribution in the past/present, the exploration of the subsurface (2 meters) and the hydrothermal alteration process along the Martian surface (Courrèges-Lacoste et al 2007). This will allow the scientific community to get a characterization of the exobiological environment and improve the knowledge of the Martian environment (Courrèges-Lacoste et al 2007). In this aspect, one of the instruments inside the analytical laboratory Drawler is the RLS (Raman Laser Spectrometer) instrument (see Figure 1-B and C), being one of the flagship instrumentations due to its capabilities. The Raman Spectroscopy advantages are bind to being a non-destructive measuring technique and it meets all the aims/objectives, geochemical issues and astrobiological issues for the ExoMars mission (Böttger et al 2012; Hutchinson et al 2014; Pérez & Martinez-frias 2006). Moreover, the vibrational, rotational and other low frequencies Raman scattering of monochromatic light from a laser can provide to the scientific community a direct identification of organic compounds - past and present - and the identification of bio-mineral products as indicators of biological activity. But the synergy of the RLS intrument with other spectroscopic instruments like MicroOmega-IR Instrument (Infrared Imaging Spectrometer), which is based on Infrared spectroscopy, is necessary to maximize and complement the future results (Lalla 2014; Pérez & Martinez-Frias 2006). Thus, the infrared technique is specially sensitive to the carbon and water signal, but MicroOmega-IR Instrument will be also responsible to obtain the geological characterization which could reveal the geological processes, weathering and environmental alteration from the past and present of Mars (Böttger et al 2012; Pilorget & Bibring 2014).

The main motivation of this research is to study the degradation of different amino acids placed on volcanic matrix bulks at different extreme conditions (Martian surface environment, space environment, etc) and its possible interaction with the alteration of mineral species during the exposition to the simulated environment achieved by the

PASC simulator chamber (Poch et al 2014). The spectroscopic techniques (Raman and IR) were selected taking into account the Raman and IR systems on the ExoMars mission, for endeavouring the use of these systems on the future space mission, and the capabilities of combined Raman-IR analyses for astrobiological targets such as biomarkers.
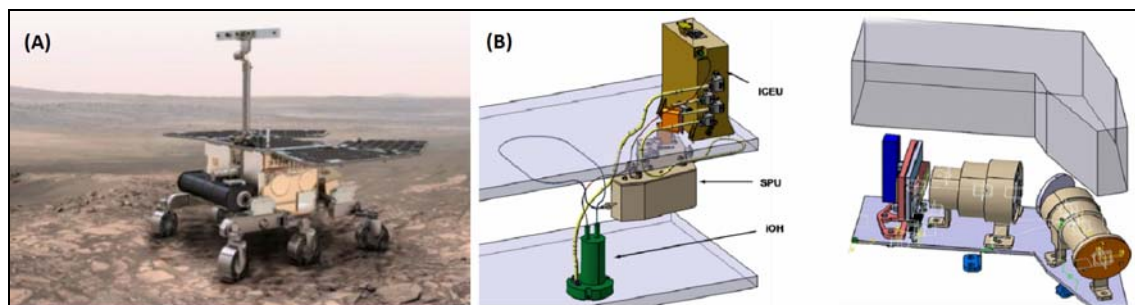

Figure 1. (A) Concept design of ExoMars Rover on Mars (Credits: ESA). (B) Design of the Raman Laser Spectrometer (Credits: ESA and INTA-Centro de Astrobiología).

Planetary Atmosphere and Surfaces Chamber (PASC). The simulation chamber PASC is composed by an UHV (ultra-high-vacuum) chamber 500 mm long and 400 mm by diameter, with standard CF flanges (Figure 2). The pressure is controlled by a Pirani-Penning combined sensor, covering a range from 1000 to $5x10^{-9}$ mbar. The base pressure of the chamber is in 10^{-10} mbar ranges. Other important parts of the chamber are the feedback steeped motor valves which control the aperture of a CF-500 turbo molecular pump changing it as pressure changes. Its main goal is to achieve conditions of relative low pressures. On the other hand, for the atmosphere simulation, a manifold is used for the required gas proportion but each gas mixture is controlled by individual flux-meters (dosing valves). The proportion of gas composition is controlled by a residual gas analyzer (RGA) mass spectrometer (quadrupole type). Then, the desired partial pressure of the gas can be monitorized by RGA and opening or closing the flux-meters manually. Previously, a calibration process has to be performed. The percentage of each gas in the atmosphere is continuously monitored in order to follow possible condensation or desorption processes as function of time, temperature or irradiation. The RGA can perform from 10^{-4} mbar to 10^{-10} mbar . To guarantee the temperature of the sample, PASC has a helium cooling system connected to the sample holder through a thermally isolated Helium transfer rod and cools down the sample. The temperature measurement is done by two silicon diodes in different parts of the sample holder and in order to warm up the sample, a 50 Ω electrical resistance is used. Thus, the sample can be stabilized from 4 to 325 Kelvin (K) (Mateo-Martí et al 2006). The amount of water can be controlled inside the chamber. It is introduced by a heater where is vaporized and sent to a gas line, then it is dragged to the chamber by the gas mixture. The sample container is made of copper with a gold coverage layer to improve the thermal conductivity. Although the sample can be positioned to be irradiated, there is instrumentation inside PASC that monitors *in situ* the chemical changes induced by an specific atmosphere. The spectroscopic technique chosen is the IR Spectroscopy (Mateo-Martí et al 2006; Mateo-Marti 2014).

The vacuum chamber has two symmetric CF windows made of SeZn and they allow the IR beam to get in and out of the simulation chamber after reflection on the sample surface.

The UV radiation is emitted by a deuterium lamp (200-400 nm) that enters through a quartz window. The UV radiation passes through a beam splitter, which passes the 88% of the radiation. The rest of the radiation is reflected to an UV detector that permits a continuous monitoring of the UV flux. After the beam splitter is passed, the UV radiation is focused by lenses on the surface of the sample. The beam splitter, lens and the beam on the surface position can be isolated from the main chamber by a valve to avoid damage of the optical system when using corrosive gasses or water vapour (Caro et al

2006; Mateo-Martí et al 2006; Mateo-Marti 2014). The *in situ* IR System is achieved by two pairs of symmetric CF windows made of SeZn, which allow the IR beam to get in and out of the simulation chamber after scattering at the sample surface. The possible incidence angles are 30° and 45° with respect to the normal sample position. Through the first window the IR beam is focused on the surface by a mirror. Once reflected on the surface, the IR beam is collected through the symmetrical window by an external focussing mirror, which focuses the reflected beam into the IR detector (Figure 2-C) (Mateo-Martí et al 2006; Mateo-Marti 2014).
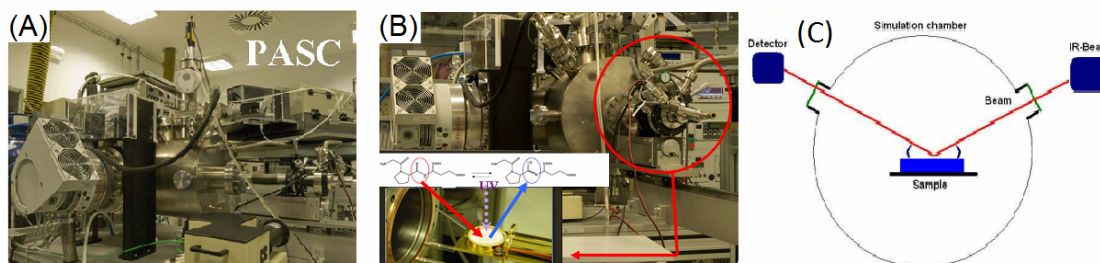

Figure 2. (A) Image of the Planetary Atmosphere and Surfaces Chamber (PASC) and planetary-simulation equipment. (B) Example of stability and chemical tautomeric transformation under UV-radiation system in PASC. (C) Schematic design of the IR spectroscopy coupled to PASC (Credits: Centro de Astrobiología-INTA-CSIC) (Mateo-Marti 2014).

***Ex situ* measurement Systems and Experimental Setup**. The 633 nm Raman data were achieved with a Micro-Raman System equipped with a 632.8 nm Electro-Optics Laser He-Ne, 10mW laser power on sample, a Kaiser OSI MKII Raman head probe coupled to a Nikon Eclipse E600 microscope and a Nikon 20x objective. The spot laser over the samples with this optical system was around 80 μm. The spectra were registered by a Kaiser OSI HoloSpec f/1.8i spectrometer equipped with a diffraction grating for Rayleigh 633 nm and an Andor CCD working at -40ºC. The Raman spectral range was from 0 to 3800 cm^{-1}, with best resolution of 5 cm^{-1}.

The infrared spectra had been obtained with a Perkin Elmer Spectrum 100 FT-IR spectrometer system equipped with a universal ATR sampling accessory. The measurement conditions were a best spectral resolution of 4 cm^{-1}, 8 accumulations, and the same samples of Raman analysis were used.

The X-ray analyses were carried out with XRD diffractometer Philips PW1710, equipped with automatic divergent slit graphite monochromator and Cu-anode. The experimental conditions achieved were: CuKα radiation, λ = 0.154nm, a niquel filter, an aluminum sample-holder, 40kV generator voltage, generator current 30 mA with a relation intensity of 0.5 (a_1/ a_2) and angle range (2θ) from 5 to 70º. The second XRD system was a Terra XRD diffractometer instrument based on the MSL-CheMin concept with a detector 1024 X 256 pixels, 2D peltier cooled CCD camera for XRD with a source cobalt X-ray tube of 30Kv-300uA was also used. For the XRD analysis a sample preparation was necessary, consisting on the powdering of a minimum part of the samples (from 2 to 4 mg) and sieved with a granulometry lower than 50 μm. Moreover, the complementary analysis with scanning electron microscopy (SEM) was performed with an ESEM-Quanta 200F Microscope. For this analysis, sample preparation was unnecessary and the measurements were directly performed on the bulk samples.

Samples preparation and Experimental Procedure. The samples set were collected by picking out samples on the studied areas on several expeditions to Tenerife Island on 2009 and 2010, being all of them catalogued and photographed using the following quotation (Table 2), taking into account the volcanic processes, alteration processes, the mineral structures and considering the possibilities as Martian analogy (see Figure 3) (Caramazana Sansano et al 2010; Lalla 2014). A total of 10 samples were selected and used (3 samples from Los Azulejos Outcrop (AZJL); 5 samples from Las Cañadas Outcrop (TNFC) and 2 samples from Las Mercedes Outcrop (TNFM))
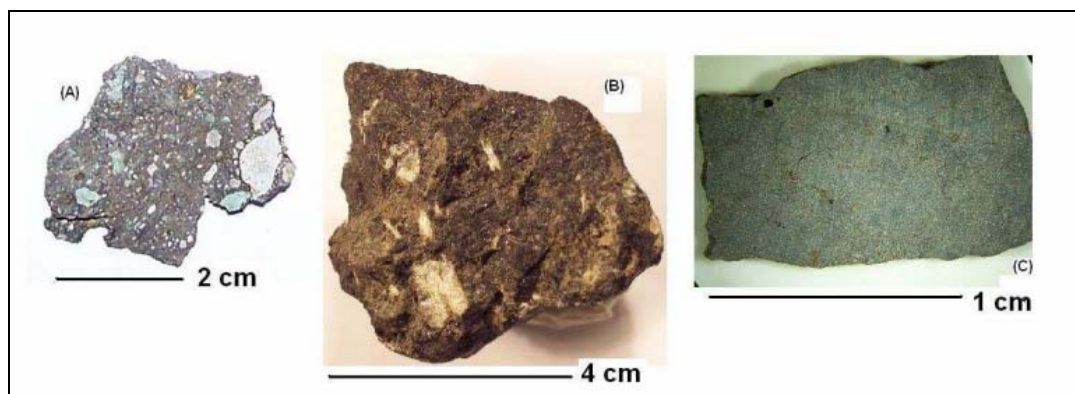
Figure 3. Pictures of some samples catalogued: (A) Samples from Los Azulejos outrocp, Tenerife, Spain (AZJL); (B) samples from Las Cañadas, Tenerife, Spain (TNFC); (C) samples from Monte de Las Mercedes, Tenerife, Spain (TFNM).

On the other hand, the amino acids chosen for the experiment have different properties depending on the chemical functional group and the site chain (Izumi et al 2008; Zhu et al 2011). The amino acids are the following: *L-aspartic acid* (abbreviation: *Asp*, chemical formula: $HOOCCH(NH_2)CH_2COOH$), *L-cysteine* (abbreviation: Cys, chemical formula: $HO_2CCH(NH_2)CH_2SH$), *L-serine* (abbreviation: Ser, chemical formula: $HO_2CCH(NH_2)CH_2OH$) and *L-alanine* (abbreviation: Ala, chemical formula: $CH_3CH(NH_2COOH)$ (Figure 4).
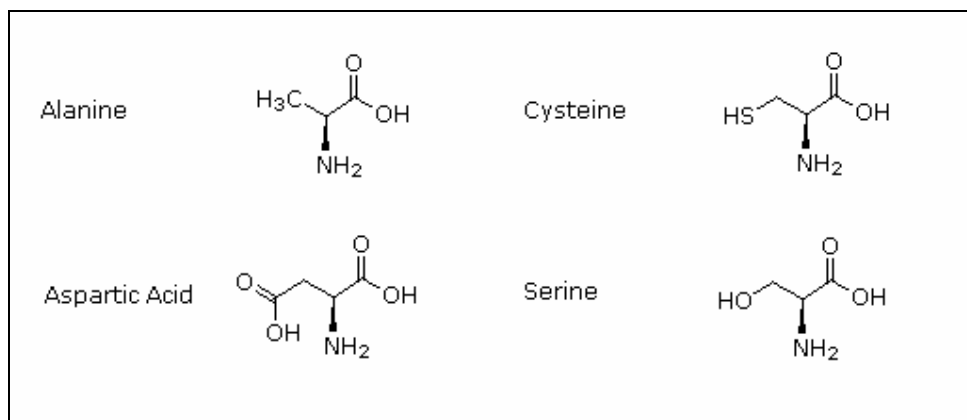

Figure 4. Chemical Structure and diagram of the amino acids.

The samples were cleaned using distilled water in order to avoid possible biological contamination from the outcrops. Once the samples were properly cleaned, the amino acids were immobilized on the host rock using distilled water solution, where 1 mg of amino acid were disolved on 50 mL water solution. The molar concentration of the different amino acids were the following: (1) *L-aspartic acid* $1,51x10^{-4}$M; (2) *L-alanine* $2,24x10^{-4}$M; (3) *L-cysteine* $1,65x10^{-4}$M; and (4) *L-serine* $1,90x10^{-4}$M.

   On the study of the amino acids immobilization, different time exposures to the dopant have been performed, where the objective was to see the grade of accumulation of the amino acid on the host rock and possible grade of interaction with the host-matrix. Moreover, the samples with different amino acids were studied by Raman spectroscopy and IR spectroscopy for choosing the most appropiate. By using Raman mapping and microscope direct observation, it was possible to detect it, and the *L-aspartic acid* (Asp) was the one with the higher concentration on the surface (see Figure 5).
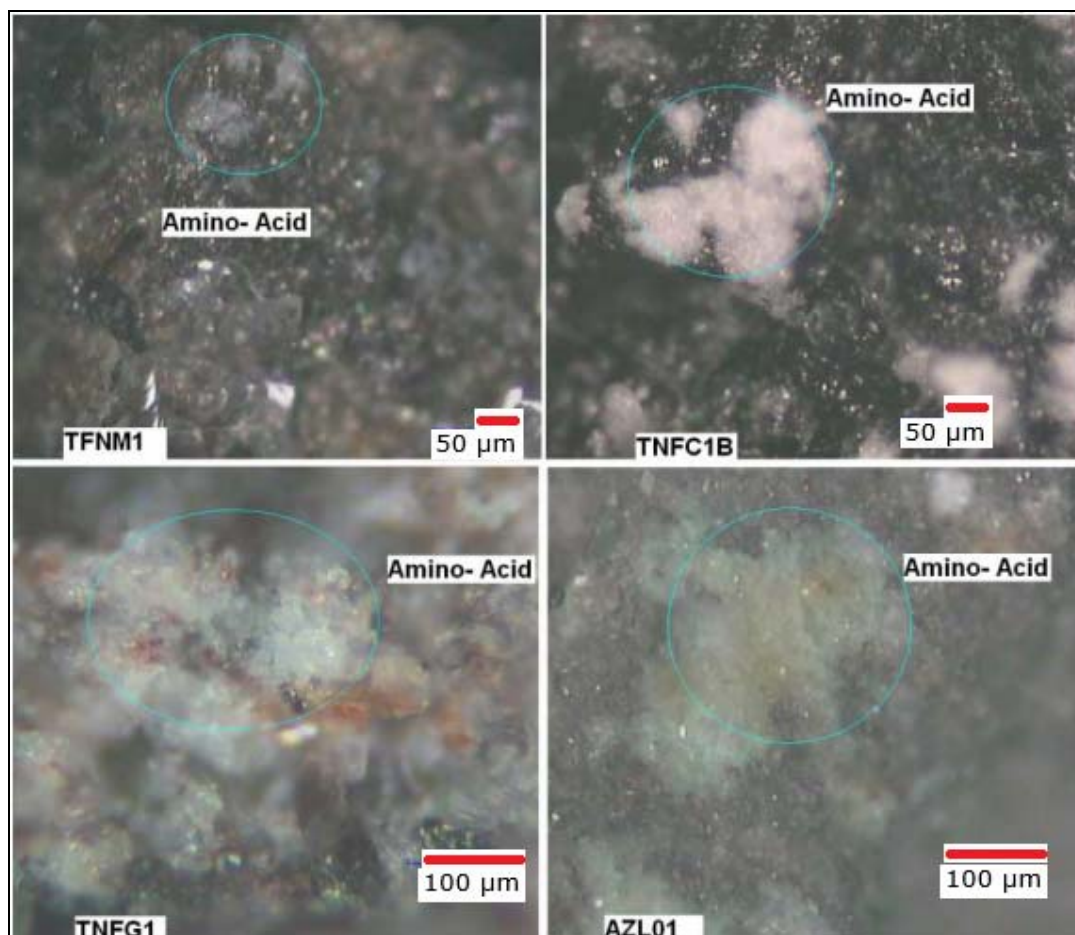
Figure 5. Pictures taken by microscopy of zone with *L-aspartic (Asp)* acid on different samples.

Different experiments were performed using the simulation chamber (PASC) trying to detect the degradation of the amino acid and the possible interaction with the host matrix for different conditions. However, the Martian conditions are the more interesting and the main motivation for this research (see Table 1). For the experiments it was necessary to obtain a 7 mbar pressure, the average atmospheric pressure of the planet. The temperature range varies from 150K to 280K for day-cycles or seasonal-cycles, but only the temperature of 180 K was applied because it covers the main objectives. The proportion of the gasses known for the Martian atmosphere at the planet surface is 95% CO_2, 2,7% N_2, 1,6% Ar, and 0,6% H_2O. Thus, it is necessary to close the valve of the main turbo pump up to 90% and to stop the entire differential pumping at the source compartment. This prevents the use of the irradiation sources in Martian atmosphere. The effect of the ionization must be done at stable atmosphere. Once the partial pressure is stable, it is necessary to cool down the surface to the desired temperature. After the temperature is stabilized, the fluctuations in the partial pressure have to be taken into account due to the heating stage, which can cause the adsorption and desorption of the molecules in the samples holder. The irradiation on the samples depends on the total gas pressure of the atmosphere and the energy of the incident particles. In this case, the atmospheric gasses absorb the incoming radiation and a small amount of electrons and ions arrive to the sample, but for the UV-radiation, it depends on the atmospheric composition and total pressure specially at wavelenght range of 400-200 nm (Mateo-Marti et al 2006). The integral UV flux achieved was taking into account the Martian flux surface in the range 190-390 nm which correspond to ~ 2.10^{15} photons cm^{-2} s^{-1} approximately (Caro et al 2006).

Summary of some samples experiment under PASC simulation Chamber. The amino acid used was the *L-aspartic acid* (Asp), due to the other amino acid did not obtain high grade of accumulation on the bulk

Sample	AA/AT	Temp	Atm	Press	UV-Rad
TNFC1B	Asp/72 hours	180K	Martian	7 mbar	4 hours
TNFC1B	Asp/2 hours	180K	Martian	7 mbar	4 hours
TNFC1B	H_2O/ 72 hours	180K	Martian	7 mbar	4 hours
TFNM1	Asp/6 days	293K	Vacuum	10^{-6} mbar	24 hours
TNFM1	No AA	293K	Vacuum	10^{-6} mbar	24 hours
AZL01	No AA	293K	Terrestrial	1000 mbar	20 minutes
AZL01	No AA	293K	Vacuum	10^{-7} mbar	18 hours

Abreviations: Absorption Time: *AA* (amino acid used) and *AT* (exposition to amino acid); Temperature: *Temp* (temperature used during the simulations); Atmosphere: *Atm* (type of atmosphere employed during the simulation); Pressure: *Press* (pressure applied on the simulations)*;* UV – Radiation Exposition: *UV-Rad* (ultraviolet irradiation time).

Results and Discussion. The complete mineralogical resume of the analyses obtained by Raman and XRD can be observed on the Table 2. The results point to a primary mineralogy composed by olivine, pyroxene and plagioclase. Moreover, secondary and alterational mineralogy have been observed. The full description of the mineralogy found can be observed on the reference, where a detailed discussion of the volcanic-mineral and alterational processes are done on the different outcrop (Lalla 2014).

Table 2

Mineral species detected in the outcrops by the different techniques
(Raman, XRD and IR)

Selected Outcrop	Mineralogy (Raman, XRD and IR)
Las Cañadas (TNFC)	oxides (magnetite, hematite, goethite, anatase, rutile, quartz, silica and ilmenite); carbonates (calcite and hydrotalcite); phosphate (apatite); pyroxenes (diopside and augite); amphiboles (actinolite); olivine (forsterite, monticellite); feldspars (anorthoclase, orthoclase, microcline, sanidine, anorthite, albite, andesine and labradorite); zeolites (phillipsite and analcime); clays (kaolinite, moscovite and illite).
Las Mercedes (TNFM)	oxides (magnetite, hematite, silica and anatase); pyroxenes (diopside and augite); olivines (forsterite, monticellite); feldspars (anorthoclase, orthoclase, microcline, sanidine, anorthite, albite, andesine and labradorite).
Los Azulejos (AZJL)	oxides (magnetite, hematite, goethite, anatase, rutile, quartz, and silica); carbonates (gregoryite); sulphates (melanterite); pyroxenes (diopside and augite); feldspars (anorthoclase, orthoclase, microcline, sanidine, anorthite, albite, oligoclase, andesine and labradorite); zeolite (analcime); clays (kaolinite, moscovite and illite)

Chemical composition (in order of appereance): magnetite (Fe_3O_4), hematite (Fe_2O_3), goethite *(a-FeO(OH))*, anatase *(TiO_2)*, rutile *(TiO_2)*, quartz *(SiO_2)*, silica *(SiO_2)*, ilmenite *(FeTiO_3)*, calcite $(CaCO_3)$, hydrotalcite *((Mg_6Al_2(CO_3)(OH)16·4(H_2O))*, gregoryite *((Na_2,K_2,Ca)CO_3))*, melanterite *(FeSO_4·7H_2O)*, apatite *(Ca_5(PO_4)_3(F,Cl,OH))*, diopside *(MgCaSi_2O_6)*, augite *((Ca,Mg,Fe)_2(Si,Al)_2O_6)*, forsterite *(Mg_2SiO_4)*, monticellite *(CaMgSiO_4)*, anorthoclase *((Na,K)AlSi_3O_8)*, microcline *(KAlSi_3O_8)*, sanidine *((K,Na)(Si,Al)_4O_8)*, anorthite *(CaAl_2Si_2O_8)*, albite *(NaAlSi_3O_8)*, oligoclase/andesine *((Na,Ca)(Si,Al)_4O_8)*, labradorite *((Ca,Na)(Si,Al)_4O_8)*, phyllipsite *((Ca,K,Na)_6(Si_{10}Al_6)O_{32}·12H_2O)*, analcime *(Na(AlSi_2O_6)·H_2O)*, kaolinite *(Al2Si_2O_5(OH)_4)*, illite *(((K,H3O)(Al,Mg,Fe)_2(Si,Al)_4O_{10}[(OH)_2,(H_2O)])* and moscovite *(KAl_2(AlSi_3O_{10})(OH)_2)*.

During the experiment, *in situ* IR spectroscopic measurements (on PASC) were carried out and the results did not showed the detection of amino acid on the matrix bulk before and during the simulations. Considering the design of the IR-system on PASC (macro-mode detection), the *in situ* IR system was only capable to detect the spectra of the volcanic bulk. The volcanic primary minerals of the host matrix absorb much of the IR wavelength, it does not have good reflectance for PASC IR System and the future experiments shall be done on monomineral compositional matrix, in order to obtain better reflectance, such as olivine, feldspars (albite) or quartz.

Furthermore, some samples were polished to obtain better result, the irregular surface mineral bulk scatter and absorb the infalling UV radiation, not allowing a good degradation of amino acids (see Figure 5-A). The polishing method applied increased the degradation of the amino acid because the UV radiation can penetrate up to 2 μm and the plane bulk will produced double degradation effect caused by the direct incident UV radiation and the aditional reflected UV flux from the plane bulk (see Figure 5-B; 5-C) (Patel et al 2002).
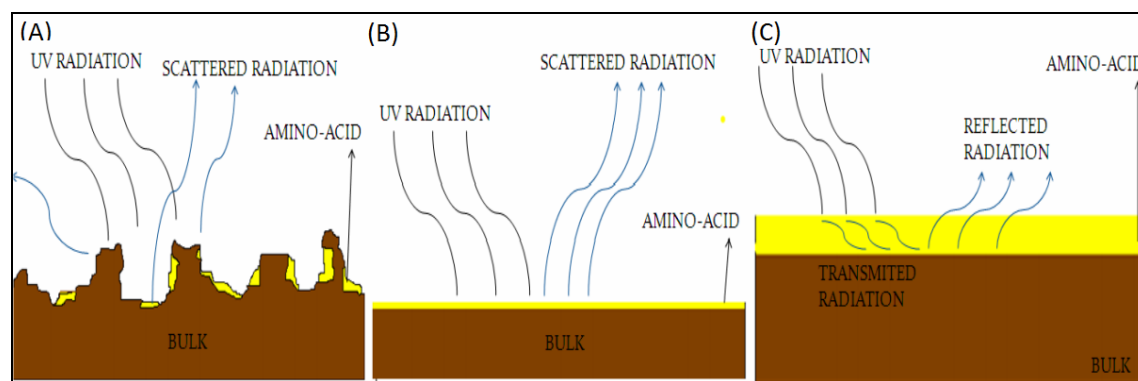

Figure 5. (A) Transversal schema of natural sample doped with the amino acid and possible action of the UV radiation, (B) transversal schema of polished doped with the amino acid and possible action of the UV radiation, (C) transversal schema of polished sample doped taking into account the direct and reflected UV light flux.

The Raman measurements were achieved in manned line mode, where 20 spectra have been measured in different parts of each sample, from the different outcrops. The dopant amino acid, before and after the immovilization process, have been fully analized and the principal vibrational Raman and infrared modes have been detected, being in accordance with the literature. The previous analyses have been done in order to avoid future possible contamination by other organic compounds during the experiment. In the case of *L-aspartic acid*, it can be observed the γ (OH) vibration at 940 cm^{-1}; the CH bending vibration at 1340 cm^{-1}; the bands at 1695 cm^{-1} and 1426 cm^{-1} assigned to the NH$_2$ and COO$^-$ stretching vibration; the C-C stretching vibration and OCO$^-$ vibration at 877 cm^{-1} and 779 cm^{-1} and the band at 2950 cm^{-1} assigned to CH$_2$ vibration (Figure 6-A) (Castro et al 1995; Zhu et al 2011).

Alfer the exposition to the simulated environment, the *L-aspartic acid* shows a clearly photo-dissociation caused by the decarboxylation photolysis process (Nikogosyan & Görner, 1995). On the Micro-Raman analyses it can be observed the dissapearance of several principal peaks. The processes can be confirmed by the band at 2950 cm^{-1}, where it shows a clear deformation and it becomes a broadening peak (see Figure 6 B-D); thus the CH$_2$ molecular bond with the rest of amino acid molecule is lost. On the other hand, the detection of OH$^-$ vibration on the Figure 6-B confirms the expected results due to the OH$^-$ bonds dissociation from the amino acid.

On the Figure 6-C, it has been detected a vibration at 1403 cm^{-1} and 1373 cm^{-1}, approximately, which cannot be correctly assigned because more peaks are necessary to distinguish and confirm the results, however they could be possible assigned to the C-N vibration, (-NH-) vibrations or CH$_3$ vibrations (Ganesan et al 2013; Sumayya et al 2008).
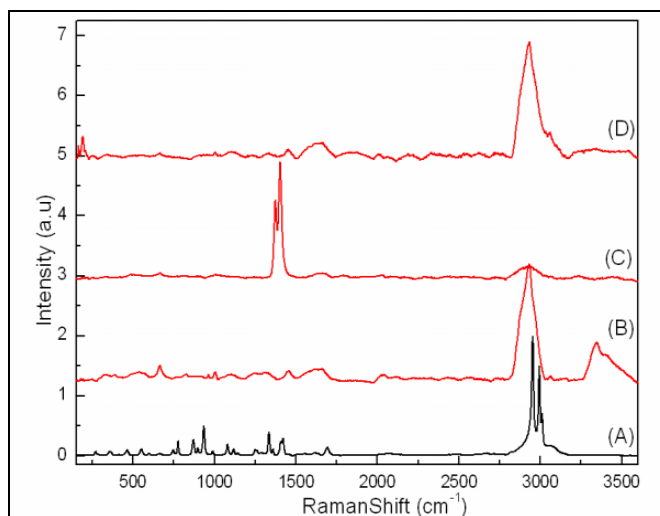
Figure 6. Raman Spectra of TNFM1 sample (Table 1). (A) TNFM1 + 6 *L-aspartic* acid exposition (B), (C) and (D) different zones of the sample TNFM01 + 6 *L-aspartic* acid exposition + simulated atmosphere.

On the *ex situ* infrared analysis (see Figure 7) at the plane host bulk matrix, it has been clearly detected the asymetric streching vibration of CH_2 at 2922 cm^{-1} and 2852 cm^{-1}, C=O stretching vibration at 1742 cm^{-1} and COO- stretching vibration at 1420 cm^{-1}, before the simulated environments. Moreover, these peaks have not been detected after the exposition to the extreme atmospherical conditions confirming the Raman analyses (Castro et al 1995).

It is important to highlight that the IR-measurements have been done in macro-mode, where some rest of the amino acid could be on the mineral surface and has not been detected due to the low quantity and it could be masked by the mineral IR-signal. In fact, the survival of the amino acid can be only observed by microscope and Scanning electron microscopy (SEM).

The SEM-EDX analyses on the different samples have been successfully achieved and they show the detection of the amino acid and its degradation by the different simulated environments (the measurement conditions are detailed on each Figure 8-A to D). Furthermore, the electronic microscopic results fully complement the Raman-IR spectroscopic measurement.
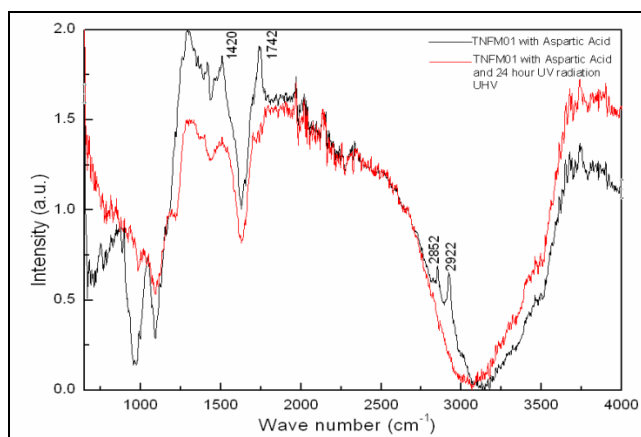

Figure 7. FTIR-ATR spectra of the TNFM1 sample. On the figure, it can be seen the samples TNFM1 with *L-aspartic acid* (black line) and TNFM1 with *L-aspartic acid* under simulated atmosphere (red line).

On the other hand, considering the relative intensities of the peaks of C and O (C/O) on the Figures B and C, it can be observed that the non-altered amino acid has relative values of 1,35 and the altered amino acid shows 0,58. However, these values have to be taken in relative sense because there is a possible contribution of the oxigen from the silicate of the matrix bulk. After several SEM measurements, the possible alteration of the mineral surface caused by the non-terrestrial conditions was not detected. Moreover, the possible interaction of the amino acids with the mineralogy of the matrix was also not confirmed.

Table 3

Different amino acid exposition to extreme environment inside PASC simulation chamber

Amino acid	Before PASC Exposition			After PASC Exposition		
	Rock Deposition	Raman Detection	Exsitu IR Detection	PASC-IR Detection	Exsitu Raman Detection	Exsitu IR Detection
L-Aspartic acid	X	X	X	O	X	X
L-Alanine	O	X	X	O	X	O
L-Cystene	O	X	X	O	X	O
L-Serine	O	X	X	O	X	O

Abreviations: X corresponds to a correct detection, where the vibrational assignment was fully achieved. O corresponds to low signal detection or not detection, where the vibrational assignment was achieved with low S/R ratio due to the adherence of amino acid to host matrix and bad IR reflectance caused by the host bulk matrix.

In the non-terrestrial environments such as the space and Martian atmospheric conditions, the photodissociation is one of the major processes causing the amino acid being broken down, creating new simple molecules in this case. However, the local conditions in closed systems such as comet or interestellar medium in combination with this proccess are capable to create new more complex molecules (Berger 2003; Commeyras et al 2004; Izumi et al 2008). In the carried experiment under PASC simulation chamber, the UV radiation and the extreme conditions dissociated the amino acid into free radicals such as CH_2^-, OH^- and C-C (Nikogosyan & Görner 1995; Sánchez et al 2012). The proposed process for the photodissociation is a photo-decarboxylation, where the HCOOH have not been detected on the Raman-IR spectra being in accordance with the references. The half-life of the amino acid shows an average time of 10^4 seconds, which is comparable to the references and to other experiments carried out in similar Planetary simulation chambers from NASA and ESA (Ten Kate et al 2005).
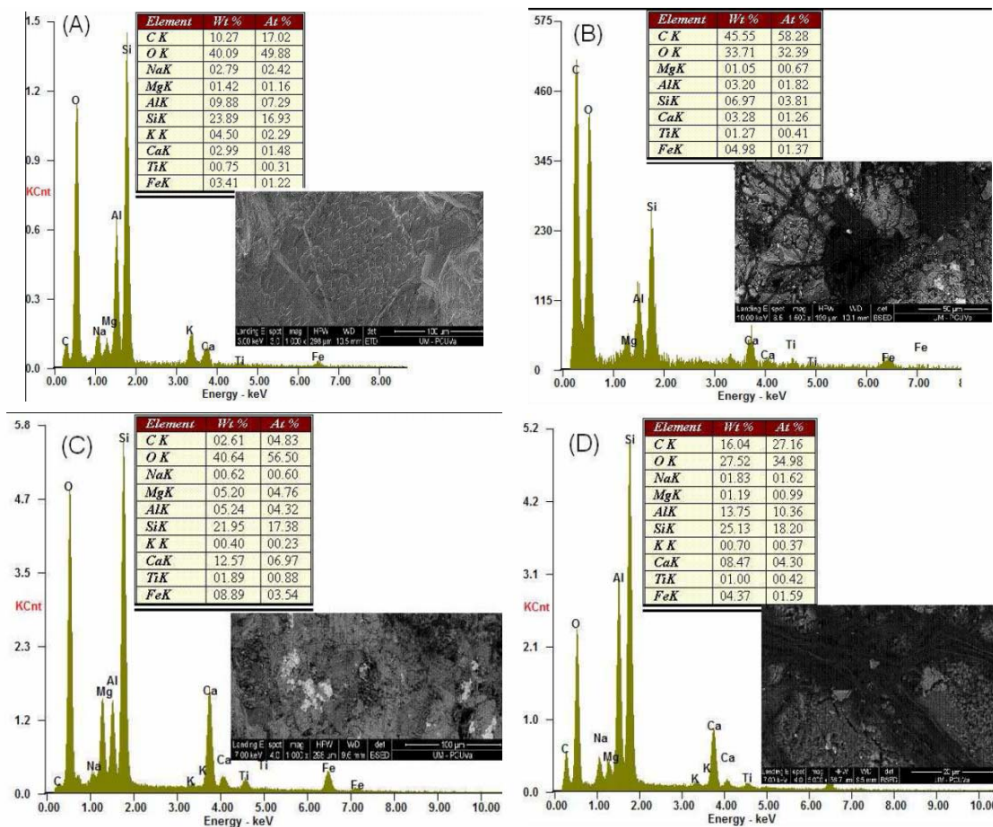
Figure 8. (A) Picture and elemental composition (by SEM-EDX) of the host matrix TFNM01 before the simulation on PASC, (B) picture and elemental composition (by SEM-EDX) of the L-aspartic acid on TFNM01 before the simulation on PASC, (C) picture and elemental composition (by SEM-EDX) of the host matrix TFNM01 after the simulation on PASC and (D) picture and elemental composition (by SEM-EDX) of the L-aspartic acid TFNM01 after the simulation on PASC in a different zone.

The results demonstrate that the organic compositions can not be stable on the Martian surface and regolith, but the free radicals can be suitable biomarkers inside the volcanic materials (Table 3). On the other hand, the stable organic material can only exist under the surface (sub-surface), where the existence of more convenient conditions, like lack of UV-radiation, hydroscopic minerals and liquid water, are achieved (Poch et al., 2013, 2014). The ESA ExoMars rover will be equipped with a driller perforation system (*Aurora-Driller*) capable to drill up to 2 meters in the subsurface, where the biological target could be successfully detected. Moreover, the *Aurora-Driller* system will be equipped with an IR spectrometer ("*Mar_Miss*"-*Mars Multispectral Imager for Subsurface*) to carry *in situ* IR measurement during the drilling process. Once the samples are obtained, they are transported to the *Drawler* Automatic Laboratory, where the Raman and IR systems will carry out the spectroscopic detailed measurements of the mineralogy and the biomarkers (Pilorget & Bibring, 2014). The micro-Raman and ATR-FTIR measurements at the "Unidad Asociada Uva-CSIC al Centro de Astrobiología-INTA-CSIC" have been able to detect the photodissociation processes on the different simulations, demonstrating that the vibrational spectroscopy is a powerful tool for the biomarkers detection and non-destructive methods (Courrèges-Lacoste et al 2007; Pérez & Martinez-Frias 2006). The IR measurements have been done in macro-mode on this research, but the MicroOmega Infrared spectrometer will work in microscopic mode with a high resolution of 20 μm × 20 μm per pixel at a few wavelengths between 0.5 μm and 0.9 μm and with a continuous and high spectral sampling from 0.9 μm to 3.5 μm. Therefore, for each pixel MicrOmega acquires the entire spectrum in a spectral domain, enabling it to identify the composition of the mineral and biological target at grain scale. Thus, IR system on ExoMars will support the scientific measurements by correlating its spectral information with other

spectroscopic and imaging instruments such as the Raman Laser Spectrometer System (Courrèges-Lacoste et al 2007; Pérez & Martinez-Frias, 2006; Pilorget & Bibring 2014).

The complementary SEM-EDX measurement has confirmed the Raman-IR results by the C/O relationship. The microscopy pictures have showed the decrease of amino acid immovilized on matrix after the simulation on PASC. Moreover, the EDX and the IR results have given new clues for future experiments related to the bulk matrix. The new measurements should be done on monomineral matrix surface with good reflectance such as pyroxene, olivine or feldspars, but also secondary materials such as zeolites, carbonates or sulphates could be considered. The C/O relation on monomineral EDX analyses could be more accurated bearing in mind that is possible to know the exact contribution of the oxigen from the matrix bulk (Lalla 2014).

Conclusions. The results agree with the references where the amino acid half–life is 10^4 seconds approximately and the amino acid at the surface has a limited stability against photolysis. However, the process is increased when the amino acid are immobilized on solid plane surface due to the fact that UV radiation can penetrate in an efficient way. The Raman and IR spectroscopy have shown to be very sensitive for the detection of organic molecules for future planetary missions as the future Raman RLS instrument and MicroOmega Infrared instrument; both techniques, working in synergy, have detected the disappearance of HCOOH and have confirmed the degradation process of amino acid (decarboxylation photolysis). The experiments have shown the versatility of the simulation chamber (PASC) in performing experiments with different planetary environment conditions. In the future, new considerations have to be done: the use of other different amino acids and mono-mineral volcanic species on the host matrix for having a better control of the possible biological-mineral processes.

References

Berger G., 2003 Deterministic hypotheses on the origin of life and of its reproduction. Med Hypotheses 61 (5–6): 586–592. doi:http://dx.doi.org/10.1016/S0306-9877(03)00237-8

Böttger U., de Vera J.-P., Fritz J., Weber I., Hübers H.-W., Schulze-Makuch D., 2012 Optimizing the detection of carotene in cyanobacteria in a martian regolith analogue with a Raman spectrometer for the ExoMars mission. Planet Space Sci 60 (1): 356–362. doi: 10.1016/j.pss.2011.10.017

Caramazana Sansano A., Sanz-Arranz A., Lalla E., García J. M., Martinez-frías J., Rull-Perez F. R., 2010 Espectroscopía Raman de Basaltos Correspondientes al Volcán de Las Arenas , Tenerife. MACLA 13 (1): 129–130.

Caro G. M., Mateo-Martí E., Martínez-Frías, J., 2006 Near-UV Transmittance of Basalt Dust as an Analog of the Martian Regolith: Implications for Sensor Calibration and Astrobiology. Sensors 6 (6): 688–696. doi:10.3390/s6060688

Castro J. L., Montañez M. A., Otero J. C., Marcos J. I., 1995 SERS and vibrational spectra of aspartic acid. J Mol Struc 349 (0): 113–116. doi: 10.1016/0022-2860(95)08722-8

Commeyras A., Taillades J., Collet H., Boiteau L., Vandenabeele-Trambouze O., Pascal R., Martin H., 2004 Chapter 5 - Molecular Origins of Life: Homochirality as a Consequence of the Dynamic Co-Emergence and Co-Evolution of Peptides and Chemical Energietics. In G. Pályi, C. Zucchi, & L. Caglioti (Eds.), Progress in

Biological Chirality pp. 49–64. Oxford: Elsevier Science Ltd. doi: 10.1016/B978-008044396-6/50007-1

Courrèges-Lacoste G. B., Ahlers B., Rull-Perez F., 2007 Combined Raman spectrometer/laser-induced breakdown spectrometer for the next ESA mission to Mars. Spectrochim Acta A 68 (4): 1023–1028. doi: 10.1016/j.saa.2007.03.026

Ganesan A., Brunger M. J., Wang F., 201 A study of aliphatic amino acids using simulated vibrational circular dichroism and Raman optical activity spectra. Eur Phys Journal D 67 (11): 229. doi:10.1140/epjd/e2013-40376-x

Gómez F., Mateo-Martí E., Prieto-Ballesteros O., Martín-Gago J., Amils R., 2010 Protection of chemolithoautotrophic bacteria exposed to simulated Mars environmental conditions. Icarus 209 (2): 482–487. doi: 10.1016/j.icarus.2010.05.027

Hutchinson I. B., Parnell J., Edwards H. G. M., Jehlicka J., Marshall C. P., Harris L. V., Ingley R., 2014 Potential for analysis of carbonaceous matter on Mars using Raman spectroscopy. Planet Space Sci 103: 184-190. doi: 10.1016/j.pss.2014.07.006

Izumi Y., Matsui T., Koketsu T., Nakagawa K., 2008 Preservation of homochirality of aspartic acid films irradiated with 8.5eV vacuum ultraviolet light. Radiat Phys Chem 77 (10–12): 1160–1163. doi: 10.1016/j.radphyschem.2008.05.012

Lalla E. A., 2014 DOCTORAL THESIS: Tenerife como análogo de Marte: Caracterización multianalítica (Raman, DRX, ATR-FTIR, SEM y MossBaeur) de muestras de interés planetario y astrobiológico. Departamento de Física de La Materia Condensada, Cristalografía Y Minerealogía - Universidad de Valladolid, 1, 217. Retrieved from http://uvadoc.uva.es/handle/10324/4572

Mateo-Marti E., 2014 Planetary Atmosphere and Surfaces Chamber (PASC): A Platform to Address Various Challenges in Astrobiology. Challenges 5 (2): 213–223. doi: 10.3390/challe5020213

Mateo-Martí E., Prieto-Ballesteros O., Sobrado J. M., Gómez-Elvira J., Martín-Gago J. A., 2006 A chamber for studying planetary environments and its applications to astrobiology. Meas Sci Technol 17 (8): 2274. Retrieved from http://stacks.iop.org/0957-0233/17/i=8/a=031

Nikogosyan D. N., Görner H., 1995 Photolysis (193 nm) of aliphatic amino acids in aqueous solution. J Photochem Photobiol B 30 (2–3): 189–193. doi: 10.1016/1011-1344(95)07187-7

Patel M. R., Zarnecki J. C., Catling D. C., 2002 Ultraviolet radiation on the surface of Mars and the Beagle 2 UV sensor. Planet Space Sci 50 (9): 915–927. doi: 10.1016/S0032-0633(02)00067-3

Pérez F. R., Martinez-Frias J., 2006 Raman spectroscopy goes to Mars. Spectroscopy Europe 18 (1): 18–21.

Pilorget C., Bibring J.-P., 2014 Automated algorithms to identify and locate grains of specific composition for (NIR) hyperspectral microscopes: Application to the MicrOmega instrument onboard ExoMars. Planet Space Sci 99 (0): 7–18. doi: 10.1016/j.pss.2014.05.017

Poch O., Kaci S., Stalport F., Szopa C., Coll P., 2014 Laboratory insights into the chemical and kinetic evolution of several organic molecules under simulated Mars surface UV radiation conditions. Icarus 242 (0): 50–63. doi: 10.1016/j.icarus.2014.07.014

Poch O., Noblet A., Stalport F., Correia J. J., Grand N., Szopa C., Coll P., 2013 Chemical evolution of organic molecules under Mars-like UV radiation conditions simulated in the laboratory with the "Mars organic molecule irradiation and evolution" (MOMIE) setup. Planet Space Sci 85 (0): 188–197. doi: 10.1016/j.pss.2013.06.013

Sánchez F. J., Mateo-Martí E., Raggio J., Meeßen J., Martínez-Frías J., Sancho L. G., De la Torre R., 2012 The resistance of the lichen *Circinaria gyrosa* (nom. provis.) towards simulated Mars conditions—a model test for the survival capacity of an eukaryotic extremophile. Planet Space Sci 72 (1): 102–110. doi: 10.1016/j.pss.2012.08.005

Sumayya A., Panicker C. Y., Tresa H., Harikumar B., 2008 Vibrational spectroscopic studies and ab initio calculations of L-glutamic acid 5-amide. RJC Rasayan J. Chem 1 (3): 548–555.

Ten Kate I. L., Garry J. R. C., Peeters Z., Quinn R., Foing B., Ehrenfreund P., 2005 Amino acid photostability on the Martian surface. Meteorit Planet Sci 40(8): 1185–1193. doi: 10.1111/j.1945-5100.2005.tb00183.x

Waiters C., 2003 To Create Space on Earth: The Space Environment Simulation Laboratory and Project Apollo. Houston, Texas: NASA Johnson Space Center.

Zhu G., Zhu X., Fan Q., Wan X., 2011 Raman spectra of amino acids and their aqueous solutions. Spectrochim Acta A 78 (3): 1187–1195. doi: 10.1016/j.saa.2010.12.079

Zorzano M. P., Mateo-Martí E., Prieto-Ballesteros O., Osuna S., Renno N., 2009 Stability of liquid saline water on present day Mars. Geophys Res Lett 36 (20): L20201. doi: 10.1029/2009GL040315

Authors:
Emmanuel Alexis Lalla, Department of Physics, Faculty of Physics, University of La Laguna, C/ Astrofísico Sánchez s/n, San Cristobal de La Laguna, Santa Cruz de Tenerife, CP 38206, Spain; e-mail: emmanuellalla@gmail.com / lallaea@cab.inta-csic.es
Eva Mateo Martí, Centro de Astrobiología CSIC-INTA associated to the NASA Astrobiology Center – Instituto Nacional de Técnica Aeroespacial, Ctra de Ajalvir Km 4, Torrejón de Ardoz, CP 28850, Madrid, Spain; e-mail: mateome@cab.inta-csic.es
Jesús Medina García, Department of Condensed Matter Physics, Crystallography and Mineralogy, Faculty of Science, University of Valladolid, C/ Dr. Mergelina, s/n, CP 47011, Valladolid, Spain. Unidad Asociada Uva-CSIC- al Centro de Astrobiología CSIC-INTA "ERICA", Av. Francisco Vallés 8, Edificio INDITI, Parque Tecnológico de Boecillo, CP 47151, Boecillo, Valladolid, Spain; e-mail: medina@fmc.uva.es
Antonio Sansano, Centro de Astrobiología CSIC-INTA associated to the NASA Astrobiology Center – Instituto Nacional de Técnica Aeroespacial, Ctra de Ajalvir Km 4, Torrejón de Ardoz, CP 28850, Madrid, Spain.
Department of Condensed Matter Physics, Crystallography and Mineralogy, Faculty of Science, University of Valladolid, C/ Dr. Mergelina, s/n, CP 47011, Valladolid, Spain.
Unidad Asociada Uva-CSIC- al Centro de Astrobiología CSIC-INTA "ERICA", Av. Francisco Vallés 8, Edificio INDITI, Parque Tecnológico de Boecillo, CP 47151, Boecillo, Valladolid, Spain; e-mail: sansanoca@cab.inta-csic.es
Aurelio Sanz-Arranz, Centro de Astrobiología CSIC-INTA associated to the NASA Astrobiology Center – Instituto Nacional de Técnica Aeroespacial, Ctra de Ajalvir Km 4, Torrejón de Ardoz, CP 28850, Madrid, Spain.
Department of Condensed Matter Physics, Crystallography and Mineralogy, Faculty of Science, University of Valladolid, C/ Dr. Mergelina, s/n, CP 47011, Valladolid, Spain.
Unidad Asociada Uva-CSIC- al Centro de Astrobiología CSIC-INTA "ERICA", Av. Francisco Vallés 8, Edificio INDITI, Parque Tecnológico de Boecillo, CP 47151, Boecillo, Valladolid, Spain; e-mail: jausanz@fmc.uva.es
Jesús Martinez-Frías, Department of Earth Dynamics and Observation, Instituto de Geociencias IGEO-(CSIC-UCM), Facultad de Ciencias Geológicas, C/ José Antonio Novais 12, Ciudad Universitaria, CP 28040, Madrid, Spain.
Unidad Asociada Uva-CSIC- al Centro de Astrobiología CSIC-INTA "ERICA", Av. Francisco Vallés 8, Edificio INDITI, Parque Tecnológico de Boecillo, CP 47151, Boecillo, Valladolid, Spain; e-mail: j.m.frias@igeo.ucm-csic.es
Fernando Rull-Perez, Centro de Astrobiología CSIC-INTA associated to the NASA Astrobiology Center – Instituto Nacional de Técnica Aeroespacial, Ctra de Ajalvir Km 4, Torrejón de Ardoz, CP 28850, Madrid, Spain.
Department of Condensed Matter Physics, Crystallography and Mineralogy, Faculty of Science, University of Valladolid, C/ Dr. Mergelina, s/n, CP 47011, Valladolid, Spain.
Unidad Asociada Uva-CSIC- al Centro de Astrobiología CSIC-INTA "ERICA", Av. Francisco Vallés 8, Edificio INDITI, Parque Tecnológico de Boecillo, CP 47151, Boecillo, Valladolid, Spain; e-mail: rull@fmc.uva.es